Polaron liquid-gas crossover at the orthorhombic-rhombohedral transition of manganites

J. A. Souza,[1,2,*] H. Terashita,[3,4] E. Granado,[3,4] R. F. Jardim,[2] N. F. Oliveira, Jr.,[2] and R. Muccillo[5]
[1]*Centro de Ciências Naturais e Humanas, Universidade Federal do ABC, 09090-900, Santo André, São Paulo, Brazil*
[2]*Instituto de Física, Universidade de São Paulo, C. P. 66318, 05315-970, São Paulo, São Paulo, Brazil*
[3]*Instituto de Física Gleb Wataghin, UNICAMP, C. P. 6165, 13083-970, Campinas, São Paulo, Brazil*
[4]*Laboratório Nacional de Luz Síncrotron, C. P. 6192, 13083-970, Campinas, São Paulo, Brazil*
[5]*Instituto de Pesquisas Energéticas e Nucleares, C. P. 11049, 05422-970, São Paulo, São Paulo, Brazil*
(Received 2 November 2007; revised manuscript received 7 June 2008; published 11 August 2008)

High-resolution synchrotron x-ray powder diffraction in $La_{0.7}Ca_{0.3}MnO_3$ shows in detail a first-order structural phase transition from orthorhombic (space-group *Pnma*) to rhombohedral (space-group $R\bar{3}c$) crystal structures near $T_S=710$ K. Magnetic susceptibility measurements show that the rhombohedral phase strictly obeys the Curie-Weiss law as opposed to the orthorhombic phase. A concomitant change in the electrical resistivity behavior, consistent with an alteration from nonadiabatic to adiabatic small polaron hopping regimes, was also observed at T_S. The simultaneous change in transport and magnetic properties are identified as a transition from a correlated polaron liquid for $T<T_S$ to an uncorrelated polaron gas for $T>T_S$, driven by the change in the crystal symmetry.

DOI: 10.1103/PhysRevB.78.054411 PACS number(s): 75.47.Lx, 75.20.−g, 72.15.Eb, 67.30.hb

I. INTRODUCTION

The microscopic mechanism underlying electronic, structural, and magnetic transitions in strong spin-lattice-charge coupled systems is a subject of great interest in condensed-matter physics.[1] Doped manganese oxides exhibiting the colossal magnetoresistance (CMR) effect as well as charge, orbital, and magnetic orderings are good examples of systems where the order parameter is believed to comprise spin, charge, and lattice degrees of freedom.[2] Double exchange[3] and electron-lattice[4] coupling theories were proposed to explain the correlation between magnetism and electronic transport. More recently, phase separation[2] and Griffiths-type singularity[5] pictures have emerged due to the presence of quenched disorder in these systems. Experimental studies have shown that correlation among order parameters originating from different degrees of freedom of electrons is the essence of the physical properties of these systems.[2,6] A better understanding of the order parameters along with the relationship between degrees of freedom may be the next step to be accomplished in this strong coupled system.

The doped manganese perovskite $La_{0.7}Ca_{0.3}MnO_3$ is believed to be a strongly coupled system bringing about unusual properties close to the ferromagnetic (FM) transition at T_c. The long-range FM transition has been characterized through thermodynamic measurements, which was shown to be continuous with a very large specific-heat exponent.[7] Neutron-scattering experiments reveal short-range FM correlations attributed to FM polarons, whose number increases rapidly as the temperature decreases to T_c.[8,9] The lack of divergence of the *magnetic* correlation length below T_c suggests a first-order phase transition.[10]

The existence of short-range magnetic correlations well above T_c is well established,[2,11] although it was not clear if there exists an upper temperature limit above which such correlations disappear. In this phase, the electronic conductivity is well described by a *small* polaron hopping mechanism.[12,13] Localized carriers are expected to polarize the ions in their neighborhood and distort the surrounding lattice, thereby exchanging energy and forming a bounded polaron. The terminology small polaron refers to the spatial extension of the lattice distortion induced by an electron or hole. Consequently, polaronic states with an extension comparable with a lattice spacing are called small polarons; large polarons are present otherwise. In a simplified approach for manganites, a small lattice polaron can be formed when an e_g electron localizes on a Mn^{3+} ion and the surrounding oxygen octahedron is distorted due to the Jahn-Teller (JT) effect. Mn^{4+} ions are JT inactive, consequently, the $Mn^{4+}O_6$ octahedra remain locally undistorted.

Structural, magnetic, and electrical conductivity studies at very high temperatures, which may disclose the complex connection between lattice, spin, and charge, are scarce in the literature. Most studies of manganese oxides have focused on the phenomena occurring below 400 K.[2] The majority of studies done above this temperature concentrates on the parent compound $LaMnO_3$, where an orbital order-disorder JT transition is observed.[14–17] This has led to difficulties in studying the critical fluctuations associated with the magnetic transition regarding the nature of the high-temperature precursors of the FM and metallic (FMM) state observed at low T.

Here, we focus on the structural, magnetic, and transport properties of $La_{0.7}Ca_{0.3}MnO_3$ in the temperature range of 300–900 K. It is known that this compound shows an orthorhombic to rhombohedral phase transition around $T_S=710$ K, which is the lowest T_S for the $La_{1-x}Ca_xMnO_3$ series.[18] Nonetheless, a detailed structural study in the high-temperature range for this composition was still lacking, to our knowledge. Our results confirm the structural phase transition from orthorhombic (*Pnma* space group) to rhombohedral ($R\bar{3}c$ space group) structures close to $T_S=710$ K and reveal a temperature interval with hysteretic behavior. The details of the crystal structure and lattice-parameter behaviors are presented. This structural transition occurring in the *paramagnetic insulating* (PMI) state provides an ideal sce-

nario for a better understanding of the evolution of the polaronic behavior through different average lattice symmetries. Our magnetic-susceptibility results indicate that the Mn spins form a classical paramagnetic state above T_S, which are in contrast to the deviations from the Curie-Weiss law found in the *Pnma* phase. Electrical resistivity measurements show a change of polaronic behavior at T_S from nonadiabatic in the *Pnma* phase to adiabatic in the $R\bar{3}c$ phase. The thermal hysteresis observed across the structural transition was also observed in our magnetic and transport measurements, unambiguously establishing the first-order nature of the structural-magneto-transport transition at T_S. Our results in conjunction with previous neutron and x-ray studies showing polaron correlations in the orthorhombic phase of related manganites point to a scenario in which the structural transition triggers a crossover between distinct electronic states that may be classified as polaron liquid and polaron gas states. Furthermore, it reveals the lattice dependent nature of polaronic precursor of the low-temperature FMM state where CMR is pronounced.

II. EXPERIMENT

A dense polycrystalline $La_{0.7}Ca_{0.3}MnO_3$ sample was prepared by the sol-gel method. The detailed procedure is explained elsewhere.[19] Magnetization measurements were performed using a Quantum Design vibrating sample magnetometer. Electrical resistivity was measured using a four-probe method using a homemade apparatus with a platinum thermometer mounted close to the sample. Silver epoxy was used to make contacts to the sample. Data were collected in air by warming to the highest temperature followed by cooling. We have performed both thermogravimetric analysis (TGA) and differential scanning calorimetry (DSC) up to 950 K (not shown) in $La_{0.7}Ca_{0.3}MnO_3$. DSC shows a robust peak at $T=710$ K indicating a phase transition. TGA revealed no changes in the studied temperature range, indicating negligible oxygen loss.

High-resolution x-ray powder-diffraction (XPD) measurements were conducted on the XPD beamline at the Laboratório Nacional de Luz Síncrotron.[20] The sintered pellet was ground and sieved to reject grains larger than ~ 5 μm. Wavelength of 1.240 Å and 2θ steps of 0.005° were chosen for our measurements. The sample holder was rocked by 1° at each step while being continuously rotated to minimize spurious graininess effects. A Ge(111) analyzer crystal was employed, yielding an instrumental resolution of ~0.01° in 2θ at low angles.[20] A furnace with Ar flow was employed for the high-temperature measurements. Rietveld refinements were carried out with the program suit GSAS (Ref. 21) and EXPGUI.[22]

III. RESULTS AND DISCUSSION

Figure 1 shows x-ray diffraction patterns collected at $T=590$ and 800 K. An orthorhombic structure with space-group *Pnma* is observed up to $T\sim 690$ K, while a rhombohedral structure with space-group $R\bar{3}c$ is observed above $T\sim 720$ K. The refined structural parameters are listed in

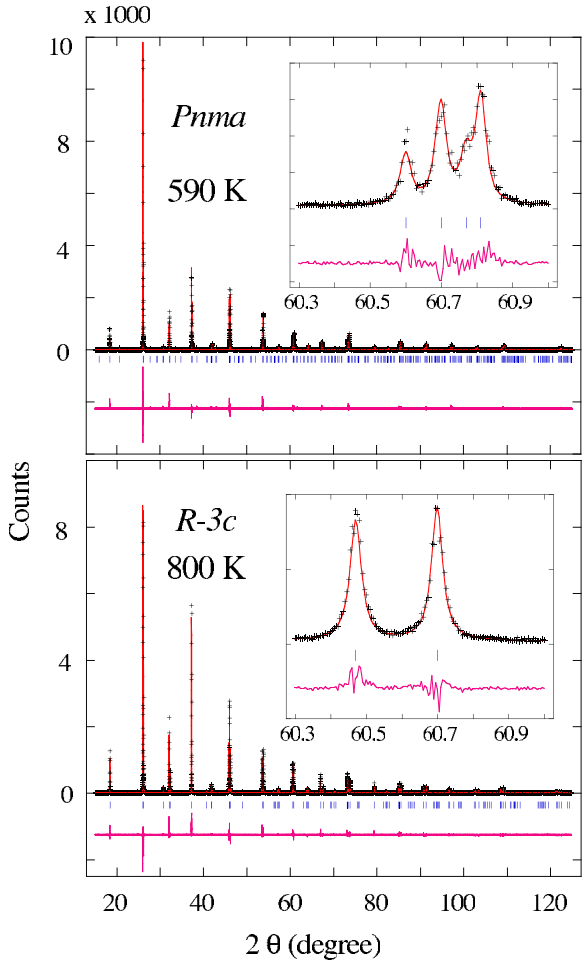

FIG. 1. (Color online) Observed (symbols), calculated (line), and difference (lower line) XPD profiles for (a) *Pnma* phase at 590 K and (b) $R\bar{3}c$ phase at 800 K. Tick marks below the patterns indicate the expected Bragg-peak positions. The insets show in detail a selected angular region of the patterns.

Table I for $T=300$, 590, and 800 K. A comparison between our refined atomic positions for the orthorhombic phase at 300 K and the corresponding parameters reported by Hibble *et al.*[23] in a neutron powder-diffraction work at this temperature reveals consistent results within three standard deviations. Figure 2 shows the temperature dependence of lattice parameters a, $b/\sqrt{2}$, c, and unit-cell volume V. For the parameters shown in this figure, a monoclinic unit-cell setting was adopted for the rhombohedral phase,[24] allowing a direct comparison with the orthorhombic lattice parameters. A discontinuity of the lattice parameters and monoclinic angle γ takes place at the orthorhombic-rhombohedral transition. This feature is more pronounced for a and b. On the other hand, the change of unit-cell volume is small and apparently continuous through the structural transition. In addition, a phase coexistence interval between $\sim T=690$ and 720 K is observed (shaded area and inset of Fig. 2). Figure 3 shows a profile illustrating the phase coexistence at 700 K. To clarify the nature of the phase transition and the evolution of the phase coexistence, we focused on this region and estimated the *Pnma* phase fraction on warming and cooling as dis-

TABLE I. Lattice and structural parameters obtained from the Rietveld refinements at 300, 590, and 800 K. Standard deviations are shown in parentheses.

Temperature (K)	300	590	800
Space group	*Pnma*	*Pnma*	$R\bar{3}c$ [a]
a (Å)	5.46632(3)	5.50030(2)	5.51251(1)
b (Å)	7.72438(3)	7.74606(3)	5.51251(1)
c (Å)	5.48111(2)	5.47725(2)	13.38826(3)
V (Å^3)	57.859(1)	58.341(1)	58.722(1)
La/Ca			
x	0.02018(13)	0.0071(3)	0
y	1/4	1/4	0
z	0.9960(2)	0.9949(3)	1/4
$U_{iso}\times 100$ (Å^2)	0.90(2)	1.14(2)	1.31(2)
Mn			
x	0	0	0
y	0	0	0
z	1/2	1/2	0
$U_{iso}\times 100$ (Å^2)	0.81(2)	0.49(3)	0.68(2)
O(1)			
x	0.4948(14)	0.469(2)	0.451(6)
y	1/4	1/4	0
z	0.0750(15)	0.0448(2)	1/4
$U_{iso}\times 100$ (Å^2) [b]	1.42(12)	3.0(2)	1.45(9)
O(2)			
x	0.2779(14)	0.2779(15)	-
y	0.0325(8)	0.0182(14)	-
z	0.7210(12)	0.730(2)	-
$U_{iso}\times 100$ (Å^2) [b]	1.42(12)	3.0(2)	-
Mn-O(1) (Å)	1.975(2)	1.960(2)	1.9621(4)
Mn-O(2) (Å)	1.959(8)	1.986(10)	-
Mn-O(2) (Å)	1.969(8)	1.923(10)	-
Mn-O(1)-Mn (°)	155.9(5)	162.4(7)	164.2(2)
Mn-O(2)-Mn (°)	160.4(3)	166.3(5)	-
⟨Mn-O⟩ (Å)	1.968(4)	1.956(5)	1.9621(4)
R_p (%)	20.3	18.3	15.5
R_{wp} (%)	27.7	24.8	20.6
χ^2	2.02	2.02	1.54

[a]Hexagonal setting was chosen.
[b]U_{iso} for O(1) and O(2) were constrained.

played in the inset of Fig. 3. A thermal hysteresis is observed. The lower panel of Fig. 2 displays the cell parameters evolution of both phases in this range as well. We therefore confirm that the nature of structural phase transition is of first order as expected.[25] In addition, any change of physical properties related to this structural transition is expected to show an equivalent thermal hysteresis associated with the phase coexistence region.

Figure 4 shows the inverse of magnetic susceptibility (χ^{-1}) corrected for the temperature independent diamagnetic and Van Vleck contributions[14] as a function of temperature.

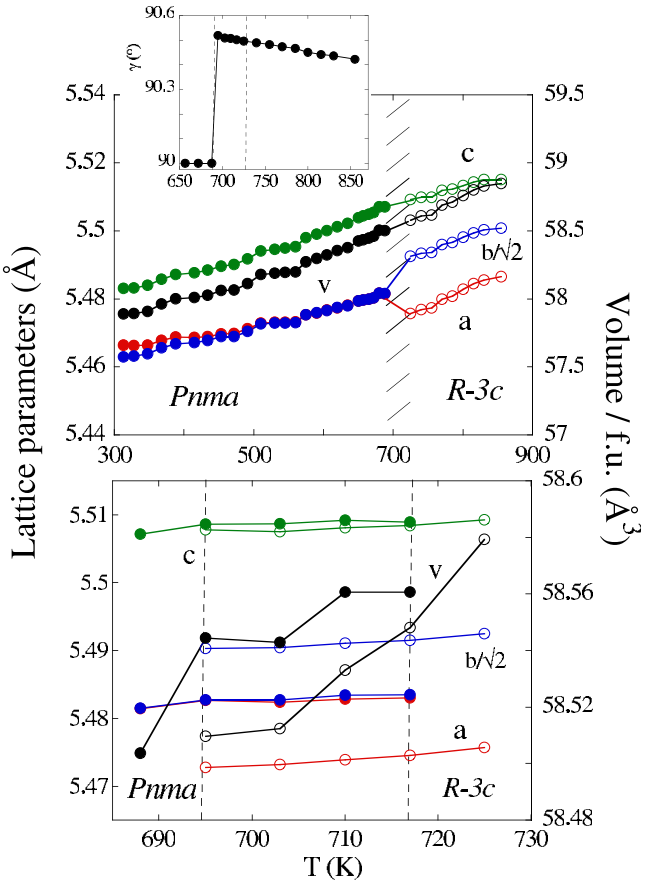

FIG. 2. (Color online) Upper panel shows temperature dependence of lattice parameters and unit-cell volume. Solid symbols and open symbols represent parameters for *Pnma* phase and $R\bar{3}c$ phase, respectively. Shaded area indicates a structural transition from an orthorhombic to a rhombohedral structure. Monoclinic coordinates were adopted for the $R\bar{3}c$ phase for a better visualization of the cell parameters evolution (Ref. 24). The monoclinic angle γ is plotted in the inset. Lower panel magnifies shaded area. Solid lines are drawn as guides to the eye.

As T is increased, two phase transitions are observed: a long-range FM transition at T_c=250 K and a hysteretic one at 710 K—clearly related to the structural transition described above. The Curie-Weiss law is obeyed *only* above T_S and the estimated effective magnetic moment is p_{eff}=4.57(3) μ_B with a Weiss temperature of θ=360 K. This agrees with the expected value (p_{eff}=4.59μ_B) for spin-only Mn ions with the appropriate Mn^{+4}/Mn^{+3} ratio, indicating that the magnetic ions are in a pure uncorrelated paramagnetic state in the rhombohedral phase. Below T_S, the slope of χ^{-1} decreases monotonically as T_c is approached from above, suggesting that spin correlations and/or a temperature-dependent exchange field arise in the orthorhombic phase. This result suggests a complex order parameter[26] induced by lattice symmetry, which will undergo a long-range FM transition at lower temperature.

The temperature dependence of the electrical resistivity ρ in this unusual paramagnetic state is shown in Fig. 5. Besides the long-range FM transition, a metalliclike phase transition along with a shrinking on the volume also sets in at T

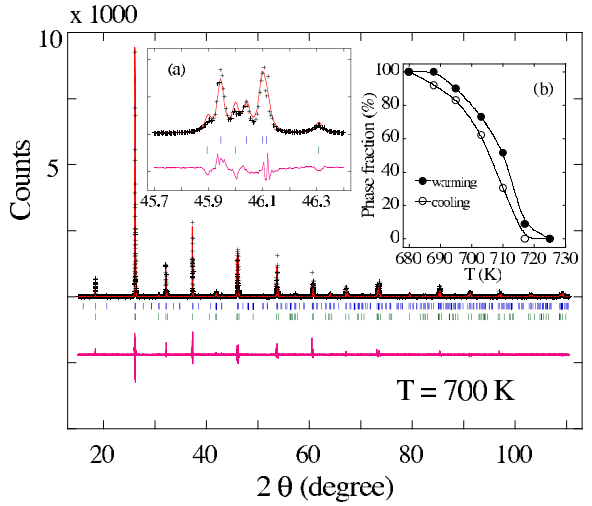

FIG. 3. (Color online) X-ray powder-diffraction profile at 700 K, where *Pnma* and $R\bar{3}c$ phases coexist. The first and second rows of thick lines indicate expected Bragg-peak positions for *Pnma* and $R\bar{3}c$ phases, respectively. The inset (a) shows well-separated Bragg peaks for both phases and (b) shows temperature dependence of phase fraction for *Pnma* phase from Rietveld refinements. Data were taken during warming (solid symbols) and cooling (open symbols). R_p=18.7%, R_{wp}=23.9%, and χ^2=2.13 were obtained.

=250 K.[27] Above this temperature, a semiconducting-like behavior $[d\rho(T)/dT<0]$ is observed in the whole studied temperature range. A sharp drop in ρ when the system undergoes the structural phase transition at $T_S \sim 710$ K is evident. The first-order character of the phase transition is again inferred from a pronounced thermal hysteresis as displayed in the inset of Fig. 5. The observed reproducibility of $\rho(T)$ in subsequent thermal runs assures that this result is not related to changes in the average oxidation state of Mn. The decrease in the electrical resistivity across T_S may be related to both a reduction in the lattice distortion (structural strain) and a change in energy gap present in the insulating state of the system. In the latter case, the higher crystallographic

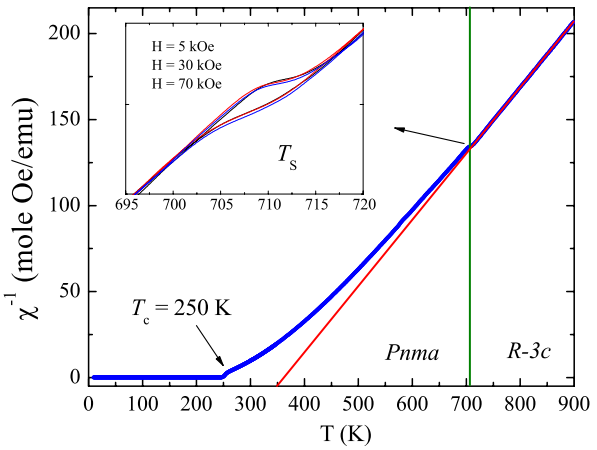

FIG. 4. (Color online) Temperature dependence of the inverse of magnetic susceptibility as a function of temperature. The inset indicates no change on the structural phase transition when magnetic fields up to 70 kOe are applied.

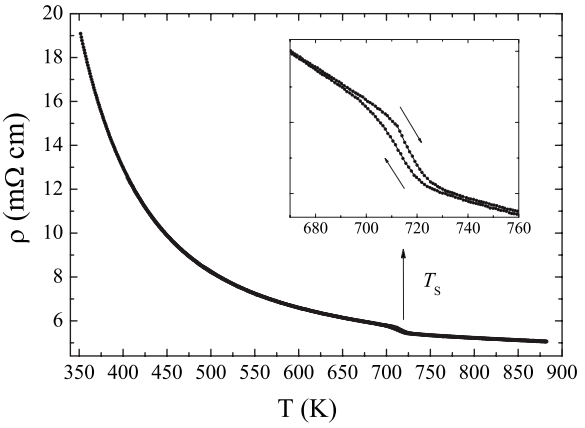

FIG. 5. Temperature dependence of the electrical resistivity. The inset shows an expanded view of the thermal hysteresis around T_S.

symmetry above T_S would decrease the gap whereby more charge carriers would be available, reducing the electrical resistivity of the system. In either case, this observation suggests that the average lattice structure plays an important role in the electronic behavior of the high-temperature PMI state.

The electrical resistivity with a small polaron model in the high-temperature PMI phase may be written as[12,13,28]

$$\rho(T) = AT^s \exp\left(\frac{E_P}{k_B T}\right), \tag{1}$$

where E_P is the polaron hopping energy and k_B is the Boltzmann constant. In the nonadiabatic limit (where $s=3/2$), the polaron is assumed to have a small probability of making a jump during each attempt period, defined as the period of oscillation for the relevant optical phonon. On the other hand, the polaron has a high probability of jumping into the next site in the so-called adiabatic approximation where $s=1$.

In Fig. 6(a), we plotted the electrical resistivity according to the adiabatic model $s=1$. It is seen that in the orthorhombic phase, the plot of $\ln(\rho/T)$ reveals a clear curvature indicating deviations from the adiabatic regime, whereas in the rhombohedral phase $\ln(\rho/T)$ shows a linear behavior consistent with small polaron hopping in the *adiabatic* regime.

In Fig. 6(b), the regime with $s=3/2$ is analyzed. In the orthorhombic phase, the linear behavior of $\ln(\rho/T^{3/2})$ indicates that the electric transport can be well described by the small polaron hopping in the *nonadiabatic* regime. From the fit, the hopping energy has been estimated to be E_P =0.19 eV. In the rhombohedral phase, $\ln(\rho/T^{3/2})$ still shows an apparent linear behavior.

It is concluded from the graphical analysis of Figs. 6(a) and 6(b) that the polaron hopping regime in the orthorhombic phase is clearly nonadiabatic. On the other hand, a more detailed analysis is necessary for the rhombohedral phase. To this end, the resistivity shown in Fig. 4 was fitted in the range 360 K$<T<$660 K for the orthorhombic phase and in the range 730 K$<T<$860 K for the rhombohedral phase using Eq. (1) with $s=1$ (adiabatic) and $s=3/2$ (nonadiabatic) and the fitting residuals were compared. For the orthorhombic phase, we obtained $\chi^2_{\text{adiab}}/\chi^2_{\text{nonadiab}}$=2.1, supporting the

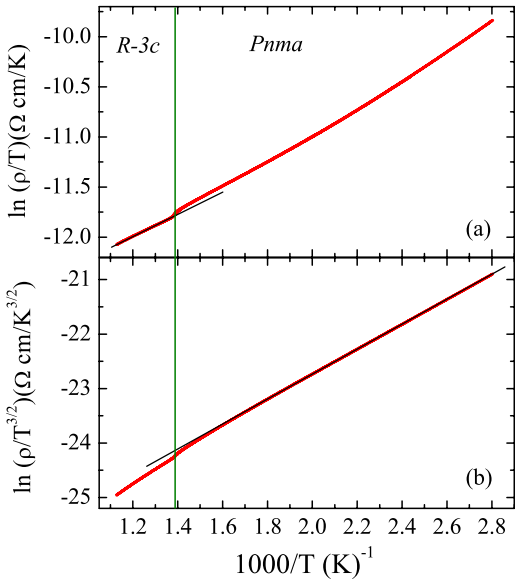

FIG. 6. (Color online) The $\rho(T)$ is plotted in the (a) adiabatic $s=1$ and (b) nonadiabatic $s=3/2$ small polaron hopping regimes. The red curve is the data and the black line is the fit.

conclusion of nonadiabatic behavior also obtained by the graphical analysis of Figs. 6(a) and 6(b). For the rhombohedral phase, we found $\chi^2_{\text{adiab}}/\chi^2_{\text{nonadiab}}=0.4$, indicating a change of behavior to the adiabatic regime. We should mention that trial fits using other models such as Arrhenius conduction and variable range hopping mechanism were done for both temperature intervals and none of these alternative models provided a good fitting to the data.

The possibility of the adiabatic polaron regime for the rhombohedral phase was further investigated by an analysis of the prefactor A in Eq. (1). In the adiabatic limit and for nondilute fractional concentration of polarons c,[12] the prefactor A in Eq. (1) is expressed as

$$A = \frac{k_B a}{g_d c(1-c)e^2 \nu_0}, \tag{2}$$

where e is the electronic charge, a is the hopping distance of the polaron, ν_0 is the relevant optical phonon frequency, and g_d is a geometrical factor.[13] The fit of our resistivity data in the rhombohedral phase according to the adiabatic model gives $A=1.71\times10^{-6}$ Ω cm/K. Inserting this value in Eq. (2) and using $c=0.7$ and $a=3.9$ Å for the average nearest-neighbor Mn-Mn distance, we obtain $g_d\nu_0=1950$ cm^{-1}. This value, when compared to the frequency of the out-of-phase stretching (JT) mode in manganites obtained by Raman scattering $\nu_0\sim600$ cm^{-1},[29] leads to $g_d\sim3$—well within the physically acceptable range between $g_d=1$ (for nearest-neighbor hopping only) and $g_d=5$ (for equal probability of nearest-neighbor and next-nearest-neighbor hopping).[13] This analysis further confirms the adiabatic regime for the rhombohedral phase of $La_{0.7}Ca_{0.3}MnO_3$. The polaron hopping energy in this phase, estimated from the $\rho(T)$ data above T_S, is $E_P=0.11$ eV, which is significantly smaller than the value found for the orthorhombic phase. This is an additional evidence that the nature of electrical transport of the small polarons depends on the lattice symmetry.

Our resistivity data may be compared to the results previously obtained by other groups. Kumar *et al.*[30] studied electrical resistivity of $La_{0.7}Ca_{0.3}MnO_3$ in the orthorhombic phase and also observed a departure from adiabatic polaron regime. The structural phase transition is absent in the high-electrical resistivity data in a series of $La_{1-x}Ca_xMnO_3$ probably due to oxygen excess.[31] More recently, Hartinger *et al.*[32] measured electrical resistivity of a thin-film $La_{0.7}Ca_{0.3}MnO_3$ sample, which agrees with small polaron conduction in high temperature. However, they only showed data up to $T\sim600$ K and consequently an electrical transport study involving the average lattice symmetry change was not discussed.

In order to rationalize the change of behavior of the magnetic susceptibility and electrical resistivity at the orthorhombic-rhombohedral transition, it is interesting to mention a number of neutron and x-ray scattering works,[8,9,33–35] which show polaronic correlations in the orthorhombic phase of several manganite compounds. Such correlations disappear in the rhombohedral phase in all studied cases.[34,36,37] It is evident that the quenching of the dynamic polaron correlations in the rhombohedral phase is closely related to the simpler magnetic and transport behaviors observed here for this phase, namely, a Curie-Weiss paramagnet polaron gas. This behavior is expected for an electronically homogeneous phase with uncorrelated polarons. On the other hand, the non-Curie-Weiss paramagnetic behavior might be due to a heterogeneous electronic state formed by a coexistence of uncorrelated and correlated polarons below T_S leading to a nonadiabatic polaron regime. In this "heavy" correlated polaron state, the hopping rate is expected to be significantly reduced. In fact, the nonadiabatic approximation is more likely to be used in the regime with higher electrical resistivity, where the hopping rate is expected to be much slower due to, for example, the greater energy gap, hopping distance, and change in the number of charge carriers (more localized character). The adiabatic limit, where the electronic motion is much faster than the ionic motion of the lattice, is assumed to be a noninteracting gas of polarons.[38] Therefore, our results naturally suggest a phase transition from a polaronic liquid (correlated) to a polaronic gas *driven by* the average lattice symmetry.

We should mention that there exists further evidence that the cooperative nature of the local distortions and long-range elastic field, which is much more pronounced in the orthorhombic phase, is responsible for changes in the strength of the charge-lattice coupling.[39] In fact, adiabatic small polaron hopping represents very well the transport mechanism above and below the high-temperature orbital order-disorder phase transition of $LaMnO_3$.[14,15] Note that in this orbital transition, the space-group symmetry is preserved. Furthermore, these results suggest that an orthorhombic lattice lowers the elastic energy for polaron correlations.

In a lower temperature range, closer to T_c, the magnetic counterpart[11] may strongly influence the electrical transport mechanism to become much more complex. We believe that this influence might be due to the fluctuations of the clustered magneticlike environment surrounding small polarons.

However, a closed analytical expression for the temperature dependence of the electrical transport including the spin degree of freedom is not available in this state. Indeed, the addition of spin interaction complicates the lattice polaron problem[40] leading to difficulties in our fundamental understanding of lattice-charge-spin coupling.[41]

IV. CONCLUSIONS

In summary, we have conducted high-resolution x-ray diffraction, magnetization, and electrical resistivity in the high-temperature PMI state of $La_{0.7}Ca_{0.3}MnO_3$. A first-order structural phase transition, from orthorhombic to rhombohedral structure, has been observed near T_S=710 K. Such a transition is accompanied by a change in the electronic conductivity from adiabatic to nonadiabatic small polaron hopping. The adiabatic regime of polaron gas is observed above T_S, where the average crystal lattice has a higher symmetry. Below T_S, the average lattice is orthorhombically distorted and it is suggested that the nonadiabatic small lattice polarons correlate each other forming a more complex polaronic structure. This picture is in agreement with magnetization results. Such a polaronic structure is believed to be a precursor of the low-temperature FMM state where CMR is pronounced. We believe that these results will impose severe constraint on any microscopic theory of the long-range orderings in intermediate and strong coupled manganites.

ACKNOWLEDGMENTS

We are indebted to J. J. Neumeier for the magnetic measurements and the useful discussion. This work was supported by the Brazilian agencies FAPESP under Grants No. 02/01856-1, No. 05/53241-9, and No. 07/01039-7 and CNPq under Grants No. 303272/2004-0 and No. 306496/1988-7.

*jasouza@if.usp.br; joseantonio.souza@ufabc.edu.br

[1] Y. Tokura, in *Colossal Magnetoresistive Oxides*, edited by Y. Tokura (Gordon and Breach, Amsterdam, 2000).
[2] E. Dagotto, T. Hotta, and A. Moreo, Phys. Rep. **344**, 1 (2001).
[3] C. Zener, Phys. Rev. **82**, 403 (1951); P. W. Anderson and H. Hasegawa, *ibid.* **100**, 675 (1955); P. G. de Gennes, *ibid.* **118**, 141 (1960).
[4] A. J. Millis, P. B. Littlewood, and B. I. Shraiman, Phys. Rev. Lett. **74**, 5144 (1995); A. J. Millis, R. Mueller, and B. I. Shraiman, Phys. Rev. B **54**, 5405 (1996).
[5] M. B. Salamon, P. Lin, and S. H. Chun, Phys. Rev. Lett. **88**, 197203 (2002).
[6] C. H. Booth, F. Bridges, G. H. Kwei, J. M. Lawrence, A. L. Cornelius, and J. J. Neumeier, Phys. Rev. Lett. **80**, 853 (1998).
[7] J. A. Souza, Yi-Kuo Yu, J. J. Neumeier, H. Terashita, and R. F. Jardim, Phys. Rev. Lett. **94**, 207209 (2005).
[8] C. P. Adams, J. W. Lynn, Y. M. Mukovskii, A. A. Arsenov, and D. A. Shulyatev, Phys. Rev. Lett. **85**, 3954 (2000).
[9] C. S. Nelson, M. v. Zimmermann, Y. J. Kim, J. P. Hill, D. Gibbs, V. Kiryukhin, T. Y. Koo, S.-W. Cheong, D. Casa, B. Keimer, Y. Tomioka, Y. Tokura, T. Gog, and C. T. Venkataraman, Phys. Rev. B **64**, 174405 (2001).
[10] C. P. Adams, J. W. Lynn, V. N. Smolyaninova, A. Biswas, R. L. Greene, W. Ratcliff, S.-W. Cheong, Y. M. Mukovskii, and D. A. Shulyatev, Phys. Rev. B **70**, 134414 (2004).
[11] J. M. De Teresa, M. R. Ibarra, P. A. Algarabel, C. Ritter, C. Marquina, J. Blasco, J. Garcia, A. del Moral, and Z. Arnold, Nature (London) **386**, 256 (1997).
[12] R. Raffaelle, H. U. Anderson, D. M. Sparlin, and P. E. Parris, Phys. Rev. B **43**, 7991 (1991).
[13] M. Jaime, H. T. Hardner, M. B. Salamon, M. Rubinstein, P. Dorsey, and D. Emin, Phys. Rev. Lett. **78**, 951 (1997); M. Jaime, M. B. Salamon, M. Rubinstein, R. E. Treece, J. S. Horwitz, and D. B. Chrisey, Phys. Rev. B **54**, 11914 (1996).
[14] J. A. Souza, J. J. Neumeier, R. K. Bollinger, B. McGuire, C. A. M. dos Santos, and H. Terashita, Phys. Rev. B **76**, 024407 (2007).
[15] P. Mandal, B. Bandyopadhyay, and B. Ghosh, Phys. Rev. B **64**, 180405(R) (2001).
[16] J. Rodriguez-Carvajal, M. Hennion, F. Moussa, A. H. Moudden, L. Pinsard, and A. Revcolevschi, Phys. Rev. B **57**, R3189 (1998).
[17] T. Chatterji, F. Fauth, B. Ouladdiaf, P. Mandal, and B. Ghosh, Phys. Rev. B **68**, 052406 (2003); T. Chatterji, D. Riley, F. Fauth, P. Mandal, and B. Ghosh, *ibid.* **73**, 094444 (2006).
[18] *Colossal Magnetoresistance Manganites*, edited by T. Chatterji (Kluwer, Dordrecht, 2004).
[19] J. A. Souza and R. F. Jardim, Phys. Rev. B **71**, 054404 (2005).
[20] F. F. Ferreira, E. Granado, W. Carvalho, Jr., S. W. Kycia, D. Bruno, and R. Droppa, Jr., J. Synchrotron Radiat. **13**, 46 (2006).
[21] A. C. Larson and R. B. Von Dreele, Los Alamos National Laboratory Report No. LAUR 84-748, 2004.
[22] B. H. Toby, J. Appl. Crystallogr. **34**, 210 (2001).
[23] S. J. Hibble, S. P. Cooper, A. C. Hannon, I. D. Fawcett, and M. Greenblatt, J. Phys.: Condens. Matter **11**, 9221 (1999).
[24] P. G. Radaelli, M. Marezio, H. Y. Hwang, and S. W. Cheong, J. Solid State Chem. **122**, 444 (1996).
[25] K. S. Aleksandrov, Ferroelectrics **14**, 801 (1976); N. W. Thomas, Acta Crystallogr., Sect. B: Struct. Sci. **54**, 585 (1998).
[26] J. A. Souza, J. J. Neumeier, and Yi-Kuo Yu, Phys. Rev. B **78**, 014436 (2008).
[27] J. A. Souza, J. J. Neumeier, and R. F. Jardim, Phys. Rev. B **75**, 012412 (2007).
[28] N. F. Mott and E. A. Davies, *Electron Processes in Non-Crystalline Materials* (Clarendon, Oxford, 1979).
[29] E. Granado, N. O. Moreno, A. Garcia, J. A. Sanjurjo, C. Rettori, I. Torriani, S. B. Oseroff, J. J. Neumeier, K. J. McClellan, S.-W. Cheong, and Y. Tokura, Phys. Rev. B **58**, 11435 (1998); M. N. Iliev, M. V. Abrashev, H.-G. Lee, V. N. Popov, Y. Y. Sun, C. Thomsen, R. L. Meng, and C. W. Chu, *ibid.* **57**, 2872 (1998).
[30] P. S. A. Kumar, P. A. Joy, and S. K. Date, J. Phys.: Condens. Matter **10**, L269 (1998).
[31] D. C. Worledge, L. Mieville, and T. H. Geballe, Phys. Rev. B **57**, 15267 (1998).

[32] Ch. Hartinger, F. Mayr, A. Loidl, and T. Kopp, Phys. Rev. B **73**, 024408 (2006).
[33] V. Kiryukhin, T. Y. Koo, A. Borissov, Y. J. Kim, C. S. Nelson, J. P. Hill, D. Gibbs, and S.-W. Cheong, Phys. Rev. B **65**, 094421 (2002).
[34] V. Kiryukhin, T. Y. Koo, H. Ishibashi, J. P. Hill, and S.-W. Cheong, Phys. Rev. B **67**, 064421 (2003); V. Kiryukhin, A. Borissov, J. S. Ahn, Q. Huang, J. W. Lynn, and S.-W. Cheong, *ibid.* **70**, 214424 (2004); V. Kiryukhin, New J. Phys. **6**, 155 (2004).
[35] J. W. Lynn, D. N. Argyriou, Y. Ren, Y. Chen, Y. M. Mukovskii, and D. A. Shulyatev, Phys. Rev. B **76**, 014437 (2007).
[36] J. F. Mitchell, D. N. Argyriou, C. D. Potter, D. G. Hinks, J. D. Jorgensen, and S. D. Bader, Phys. Rev. B **54**, 6172 (1996).
[37] J. Mira, J. Rivas, L. E. Hueso, F. Rivadulla, M. A. Lopez Quintela, M. A. Senaris Rodriguez, and C. A. Ramos, Phys. Rev. B **65**, 024418 (2001).
[38] T. Holstein, Ann. Phys. (N.Y.) **8**, 325 (1959); D. Emin and T. Holstein, *ibid.* **53**, 439 (1969).
[39] D. I. Khomskii and K. I. Kugel, Phys. Rev. B **67**, 134401 (2003).
[40] R. P. Feynman, Phys. Rev. **97**, 660 (1954); R. P. Feynman, R. W. Hellwarth, C. K. Iddings, and P. M. Platzman, *ibid.* **127**, 1004 (1962).
[41] D. Emin, M. S. Hillery, and Nai-Li H. Liu, Phys. Rev. B **35**, 641 (1987); D. Emin and M. S. Hillery, *ibid.* **37**, 4060 (1988).